Molecular Diversity
https://doi.org/10.1007/s11030-023-10712-9

ORIGINAL ARTICLE

A green one-pot synthetic protocol of hexahydropyrimido[4,5-*d*] pyrimidin-4(1*H*)-one derivatives: molecular docking, ADMET, anticancer and antimicrobial studies

Harsh D. Trivedi[1] · Bonny Y. Patel[2] · Sanjay D. Hadiyal[3] · Gopal Italiya[4] · Prasanna Srinivasan Ramalingam[4]

Received: 22 June 2023 / Accepted: 7 August 2023

Abstract

Ten hexahydropyrimido[4,5-*d*]pyrimidine derivatives have been synthesized by using a green and time-efficient microwave method. The synthesized motifs were evaluated for their anticancer activity, antimicrobial activity, molecular docking, drug likeliness and ADMET studies. Comparatively, the hetero-aromatic pyrazole substituted compound **4a** exhibited the highest anticancer activity [Mean growth percent: 35.57], while EDG [$-N(CH_3)_2$] substituted compound **4i** indicated very good activity [Mean growth percent: 60.92] against various cell lines. From the computational studies, Compound **4a** passed the drug-likeness and ADME properties, fewer toxic properties, and potent inhibitory potential against the RIPK2 with significant binding affinity. In-silico molecular docking revealed that the compound **4a** has significant binding energy (− 9.8 kcal/mol) and dissociation constant (0.54 µM) properties. Additionally, synthesized motifs were evaluated for antimicrobial activity by MIC referencing the standards. According to the SAR evaluations, the compounds **4f** (4-NO_2), **4g** (3-NO_2), and **4h** (2-Cl) that include EWGs substituted aldehydes performed well as antimicrobials against selected bacterial and fungal strains. Thus, the synthesized pyrimido[4,5-*d*]pyrimidine with the heterocyclic and EWGs substituents could act as a potential candidate after further structural optimization for anticancer and antimicrobial drug discovery, respectively.

Graphical abstract

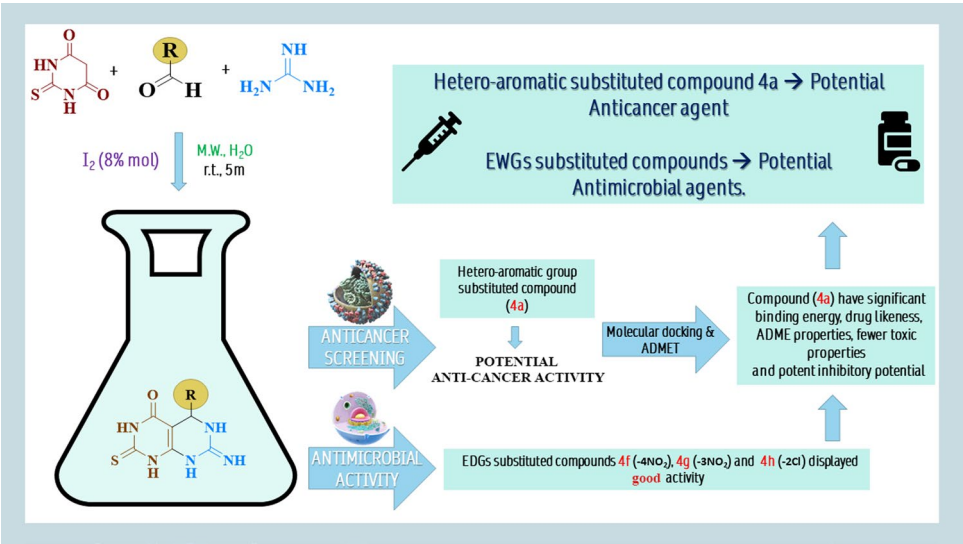

Keywords Pyrimido[4,5-*d*]pyrimidine · Green synthesis · Anticancer · Antimicrobial · Molecular docking · ADMET

Extended author information available on the last page of the article

Published online: 11 August 2023

Abbreviations

ADME	Absorption, distribution, metabolism and excretion
EWG	Electron withdrawing group
EDG	Electron donating group
WHO	World Health Organization
R&D	Research and development
NMR	Nuclear magnetic resonance
FT-IR	Fourier transform infrared spectroscopy
LC–MS	Liquid chromatography–mass spectrometry
NCI	National Cancer Institute

Introduction

Cancer is one of the leading reasons of death worldwide and is anticipated to remain the chief mortality aspect in the future [1]. Negative lifestyle, food habits and environmental factors cause up to 90% of cancer cases, so cancer can also be termed a lifestyle disease [2]. As per the world cancer report released by WHO, the mortality rates due to cancer disease will be higher, approximately twice its current percentage in the forthcoming years [3]. It has been a huge challenge for the scientists who deal with medicinal chemistry in the upcoming with the identification of novel lead analogues which can be utilized to design less toxic and highly active anticancer agents. Despite the considerable advancements made in the R&D of various cancer static medicines over the last decades, there are still two major drawbacks of modern antitumor chemotherapy including, the selectivity of conventional chemotherapeutic agents for cancer tissues with their unwanted side effects and multiple drug resistance properties of cancer cells. [4] Unwanted side effects of antitumor drugs could be overcome with capable agents who can discriminate tumor cells from normal proliferative cells and the resistance could be minimized using a combined modality approach with various complementary mechanisms of action [5]. In recent years, microbial resistance and the emergence of new pathogens are also being a critical global problem that demands a critical necessity to design and develop new antimicrobial agents which are more potent compared to marketed drugs [6–9]. *N*-Heterocycles having versatile bio-applications can be the optimum solution to tackle this type of vast issues [10–19]. Designing hybrid entities by uniting two or more bio-active heterocycles in a sole structural skeleton can up-bring potency so it could be the best approach to tackle this type of gigantic problem [20–22]. Pyrimidines are essential components of DNA and RNA, making them of the greatest significance in chemical and pharmaceutical chemistry [23]. Pyrimido[4,5-*d*]pyrimidines is the combination of two fused pyrimidine rings exhibit vivid pharmacological activities [24, 25].

The application of microwave-assisted organic reactions has benefited significantly in organic chemistry [26]. The timeless ease of workability and the eco-friendly condition is the reason that microwaves deliver an alternative to eco-hazardous and objectionable procedures. The microwave irradiation method expands multiple conveniences to carry out synthesis including greener chemistries, lesser reaction time and yield amplifications. Because of the higher selectivity, swift transport of energy, sterling products, practical simplicity, and microwave irradiation-assisted syntheses have a greater advantage compared to conventional syntheses [27, 28]. Multicomponent reactions (MCRs) are one-pot processes that, play an important role in medicinal chemistry as they are inexpensive, less time-consuming and eco-friendly in comparison to conventional multistep synthesis and also furnish products with a high degree of chemical and structural variability [29, 30]. Alongside, the utilization of water as a solvent in a reaction has also received considerable attention as a green solvent due to its advantages such as being nontoxic, readily available, inexpensive and harmless [31]. We as a research group targeted synthesizing pyrimido[4,5-*d*]pyrimidines by green, simple and time-saving reaction to utilize them as potential lead compounds for anticancer and antimicrobial drug discovery.

Results and discussion

Chemistry

This study aimed to synthesize fused pyrimido[4,5-*d*]pyrimidine derivatives with the help of a green procedure. Ten pyrimido[4,5-*d*]pyrimidine derivatives were synthesized by simple one-step green synthesis using water solvent and microwave irradiation method (Fig. 1). The mixture of 2-thiobarbituric acid, guanidine and various aldehyde derivatives in the presence of 8 mol% I_2 catalyst were placed in a microwave for 5 min. Then, the solid product was separated and washed thoroughly with sodium thiosulphate solution followed by sodium bicarbonate and water. All ten synthesized derivatives were obtained in a very good amount of yield proportions (82–93%).

Each compound was characterized by ^{1}H NMR, ^{13}C NMR, FTIR and LCMS techniques to confirm the proposed structure. The IR spectrum of compounds **4a–j** showed strong absorption band at 1502–1705 cm^{-1} due to carbonyl group. Moreover, strong absorption band at 1101–1504 cm^{-1} indicated the C–N linkage present in rings. In ^{1}H NMR spectra, the appearance of singlet peaks in compounds **4a–j** at $\delta = 10.41–11.81$ ppm was due to the proton of –N<u>H</u> located near carbonyl group. While singlet peaks at $\delta = 1.71–2.33$ ppm was because of proton of –N<u>H</u> located next to –R group. The appearance of singlet peaks of

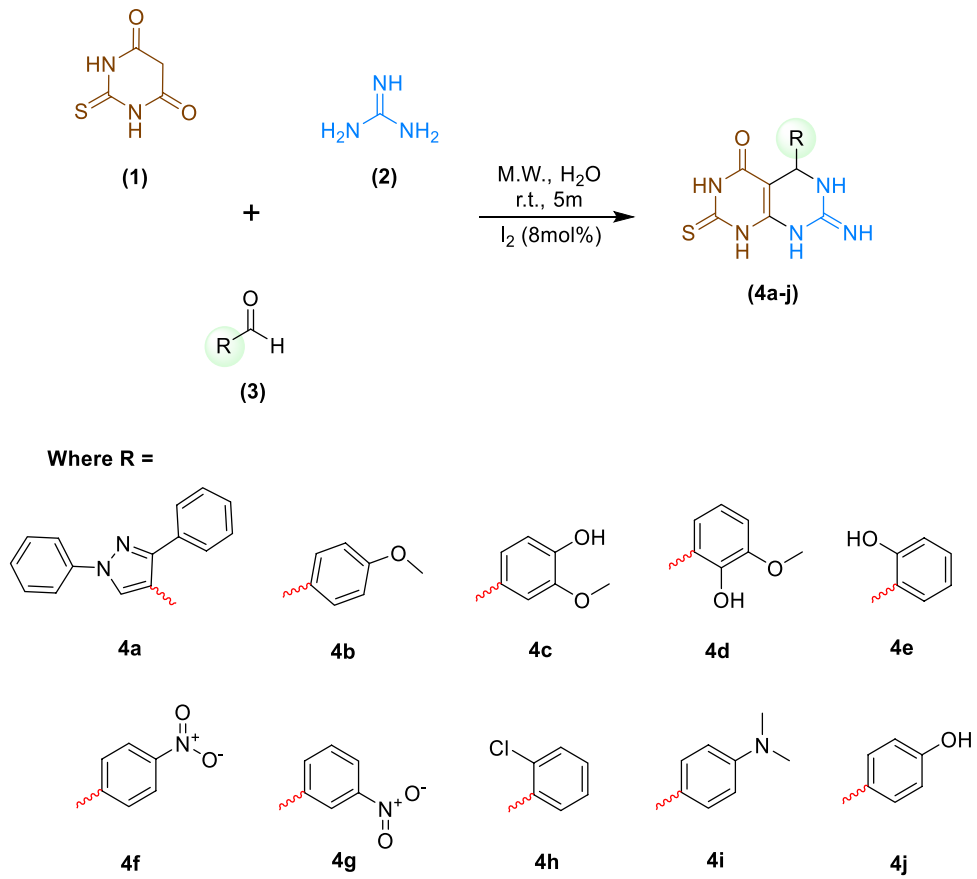

Fig. 1 Synthetic pathway for the preparation of **4a–j** derivatives

proton of =NH is at δ = 3.51–4.13. Singlet of OH peak was at 3.51, 5.98, 4.12 and 3.62 ppm of compounds **4c**, **4d**, **4e** and **4j** respectively. Similarly, signals due to protons of CH_3 of compounds **4b**, **4c**, **4d** and **4i** appeared at 3.89, 3.81, 4.13 and 2.92 respectively. The ^{13}C NMR spectrum of compounds showed characteristic signal at δ = 152.22–155.74 ppm was due to C=NH carbon. Signal of ^{13}C NMR due to carbon of C=S was appeared at under the influence of a strong electronegative environment appeared downfield at δ = 174.24–174.33 ppm. The signal of carbonyl carbon of all compounds appeared at δ = 153.04–153.34. The mass spectrums of compounds **4a–j** displayed respective molecular ion peaks in agreement with its proposed structure. Also, the spectral values for all the compounds and C, H, N analysis are presented in the experimental part.

Green metrics evaluation

The assemblage of green metrics was obtained i.e., the lower values of mass intensity and higher values of atom economy and reaction mass efficiency. The lower mass intensity values (1.32–1.43) and higher atom economy as well as mass productivity values of all synthesized compounds recognized the proposed protocol as an ideal green and sustainable approach (Table 1).

Table 1 Green metrics evaluation data

Compounds	Atom economy (%)	Mass intensity	Mass productivity
4a	91.98	1.43	69.93
4b	89.31	1.42	70.42
4c	89.79	1.32	75.75
4d	89.79	1.32	75.75
4e	88.85	1.32	75.75
4f	89.50	1.37	74.62
4g	89.50	1.40	71.42
4h	89.44	1.34	74.62
4i	89.70	1.32	75.75
4j	88.85	1.43	69.93

Biology

Anticancer evaluation

All the synthesized compounds (**4a–j**) were submitted to NCI, USA for single dose (10^{-5} M) evaluation. The growth percentage of the treated cells at 10^{-5} M concentration of all compounds is displayed in Table 2. The in-vitro anticancer primary screening studies indicated that compound **4a**

Table 2 Anticancer screening data

Entry	Cancer type	Active cell lines	Growth percent	Mean growth percent
4a	**L**	**CCRF-CEM**	**− 18.55**	**35.57**
		RPMI-8226	**− 13.96**	
	NSCLC	**NCI-H522**	**− 26.52**	
	CC	**HCT-15**	**− 46.37**	
	CNSC	**SF-539**	**− 7.75**	
	M	**LOX IMVI**	**− 86.28**	
	OC	**IGROV1**	**− 18.33**	
	RC	**RXF 393**	**− 42.16**	
	BC	**MDA-MB-468**	**− 48.92**	
4b	NSCLC	NCI-H522	80.45	104.21
4c	NSCLC	HOP-62	89.39	105.54
4d	BC	MCF7	92.02	105.52
4e	NSCLC	HOP-62	89.85	107.01
4f	RC	CAKI-1	90.20	104.87
4g	CNSC	SNB-75	84.08	103.18
4h	M	LOX IMVI	56.53	106.44
4i	**CC**	**HCT-15**	**− 43.69**	**60.92**
	M	**LOX IMVI**	**− 81.63**	
	RC	**RXF 393**	**− 19.45**	
4j	M	LOX IMVI	85.37	104.36

L leukemia, *NSCLC* non-small cell lung cancer, *CC* colon cancer, *CNSC* central nervous system cancer, *OC* ovarian cancer, *RC* renal cancer, *BC* breast cancer, *M* melanoma

Negative Growth percent and Mean growth percent <100 were selected as a significance for good activity

was found to be an effective anticancer agent against almost every tested cancer cell line i.e., CCRF-CEM (L), RPMI-8226 (L), NCI-H522 (NSCLC), HCT-15 (CC), SF-539 (CNSC), LOX IMVI (M), IGROV1 (OC), RXF 393 (RC), MDA-MB-468 (BC) with 35.57 mean growth. Moreover, compound **4i** exhibited good activity against HCT-15 (CC), LOX IMVI (M), and RXF 393 (RC) cancer cell lines. Synthesized compounds except **4a** and **4i** had displayed moderate to poor growth percentages toward the various cancer cell lines. The mean graph plots of growth percent values (one-dose graphs) are given in the supplementary material (Figs. 41–50). The graphical representation of the anticancer data is depicted in Fig. 2.

Antimicrobial evaluation

Data obtained from the antimicrobial screening result suggested that the synthesized compounds exhibited high to low activity against all the tested microbial strains compared to standard drugs (Table 3). Among the tested bacterial strains, compounds **4f** and **4h** displayed good activity against *Escherichia coli* and *Staphylococcus epidermidis*. Compound **4g** exhibited good activity against *Streptococcus pyogenes*. On the other hand, within tested fungal strains, compound **4f** indicated good activity against *Fusarium solani* while compounds **4g** and **4h** displayed good activity against *Aspergillus niger*. Other synthesized compounds revealed moderate to weak activity against tested microbial strains.

Computational study

In-silico molecular docking analysis

The binding energies (kcal/mol), dissociation constant Ki (μM) of the reference and synthesized compounds and the interacting residues of RIPK2 with these compounds

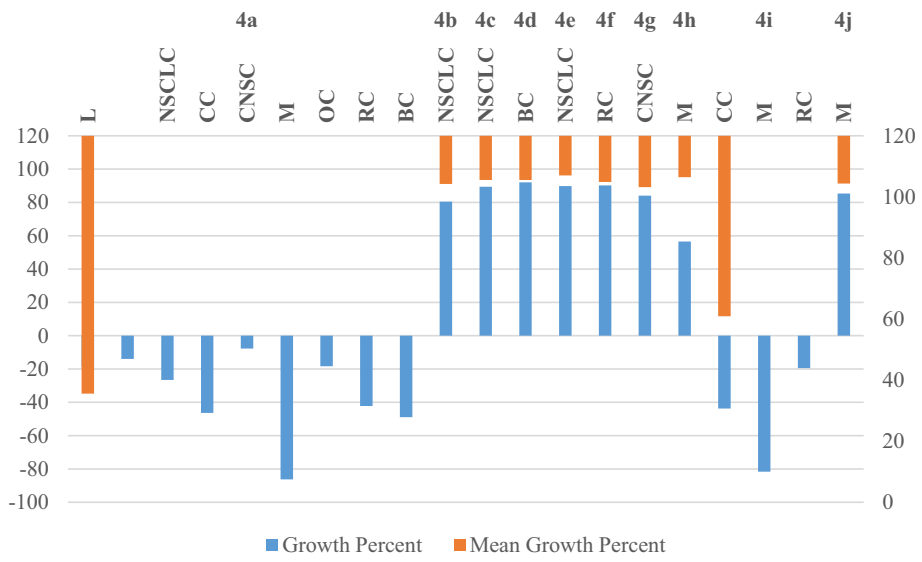

Fig. 2 Graphical depiction of anticancer evaluation data

Table 3 Antimicrobial screening data

Code	Minimum inhibitory concentration (µg/mL)					
	Bacterial strains				Fungal strains	
	E. coli	*S. marcescens*	*S. epidermidis*	*S. pyogenes*	*A. niger*	*F. solani*
4a	1500 ± 4.5	1500 ± 5.5	1500 ± 5	1500 ± 4.5	1500 ± 5	1500 ± 5.5
4b	700 ± 4	600 ± 3.5	600 ± 3	600 ± 4.5	800 ± 5	800 ± 4.5
4c	1000 ± 5.5	1000 ± 5	1000 ± 5.5	1200 ± 4.5	800 ± 3.5	800 ± 3.5
4d	1500 ± 3.5	1500 ± 4.5	1500 ± 4	1500 ± 3.5	1600 ± 3	1200 ± 4.5
4e	1200 ± 5.5	1200 ± 6	1200 ± 4.5	1200 ± 6.5	2000 ± 6	1600 ± 4
4f	**25 ± 0.5**	50 ± 0.5	**12.5 ± 0.5**	100 ± 1.5	500 ± 3.5	**50 ± 1.5**
4g	100 ± 3.5	250 ± 3.5	100 ± 2	**25 ± 1.5**	**25 ± 1.5**	250 ± 4
4h	**12.5 ± 0.5**	100 ± 2.5	**50 ± 1.5**	100 ± 3.5	**50 ± 1**	500 ± 4.5
4i	1500 ± 4.5	1500 ± 4.5	1500 ± 5	1500 ± 5.5	1500 ± 3.5	1600 ± 4
4j	900 ± 4.5	900 ± 3.5	900 ± 5	900 ± 3.5	2000 ± 5.5	1600 ± 5.5
Chloramphenicol	20 ± 1	20 ± 2	20 ± 1.5	20 ± 1	–	–
Ciprofloxacin	1 ± 0.5	0.5 ± 0.25	1.5 ± 0.5	1 ± 0.5	–	–
Nystatin	–	–	–	–	50 ± 3	100 ± 5

n = 3; values are given in mean ± SD

Table 4 Binding energies of the synthesized compounds

Compound	Binding energy (kcal/mol)	Ki (µM)	Interacting residues
Reference	− 9.83	1.23	LEU24, SER25, VAL32, ALA45, LYS47, LEU70, LEU79, ILE93, THR95, GLU96, TYR97, MET98, GLY101, GLU105, GLN150, ASN151, LEU153, ALA163, ASP164
4a	− 9.8	0.54	LEU24, SER25, GLY27, VAL32, ALA45, LYS47, GLU66, LEU70, LEU79, ILE93, THR95, GLU96, TYR97, MET98, SER102, GLN150, ASN151, ILE152, LEU153, ALA163, ASP164
4b	− 7.79	1.95	ALA45, VAL46, LYS47, GLU66, LEU70, LEU79, ILE93, VAL94, THR95, GLU96, TYR97, MET98, GLY101, LEU153, ALA163, ASP164
4c	− 7.12	6.09	LEU24, VAL32, ALA45, VAL46, LYS47, GLU66, LEU70, LEU79, ILE93, VAL94, THR95, GLU96, TYR97, MET98, GLY101, LEU153, ALA163, ASP164
4d	− 7.51	3.14	VAL42, GLN43, VAL44, LEU82, GLU96, TYR97, MET98, PRO99, ASP155, ASN156
4e	− 8.1	1.35	VAL42, GLN43, VAL44, LEU82, THR95, GLU96, TYR97, MET98, PRO99, ASP155, ASN156, LYS161
4f	− 7.31	4.42	VAL32, ALA45, VAL46, LYS47, GLU66, LEU70, LEU79, ILE93, VAL94, THR95, GLU96, TYR97, MET98, GLY101, LEU153, ALA163, ASP164
4g	− 7.15	5.73	TYR97, PRO99, ASN100, GLY101, GLU105, ARG109, GLU112, TYR113, PHE158, LYS310, LYS313
4h	− 7.37	3.96	SER25, VAL32, LYS47, GLU66, LEU79, THR95, SER102, GLN150, ASN151, ILE152, LEU153, ALA163, ASP164,
4i	− 6.65	13.36	LEU24, SER52, ALA45, TYR97, MET98, PRO99, ASN100, GLY101, GLU105, TYR113, LEU153, LYS313
4j	− 6.78	10.63	VAL32, ALA45, VAL46, LYS47, GLU66, LEU70, LEU79, ILE93, VAL94, THR95, GLU96, TYR97, MET98, GLY101, LEU153, ALA163, ASP164

were provided in Table 4. Generally, the compounds showing higher negative binding energies and low Ki values are highly preferred because of their potential binding energies toward the target protein [32, 33]. The reference (CSLP18) and synthesized compounds showed significant binding energies (− 9.8 to − 6.65 kcal/mol) with low Ki towards RIPK2. The docking results revealed that compound **4a** was shown similar binding energy (− 9.8 kcal/mol) and Ki (0.54 µM) as the reference compound which showed − 9.83 kcal/mol binding energy and 1.23 µM Ki respectively. It was also clearly evident that compound **4a** has nearly twofold decreased activity (Ki = 0.54 µM) as of the reference compound (Ki = 1.23 µM). The surface view & cartoon view of protein–ligand binding patterns of **4a** in comparison with the reference compound was shown in Fig. 3, and the protein–ligand interactions of **4a**

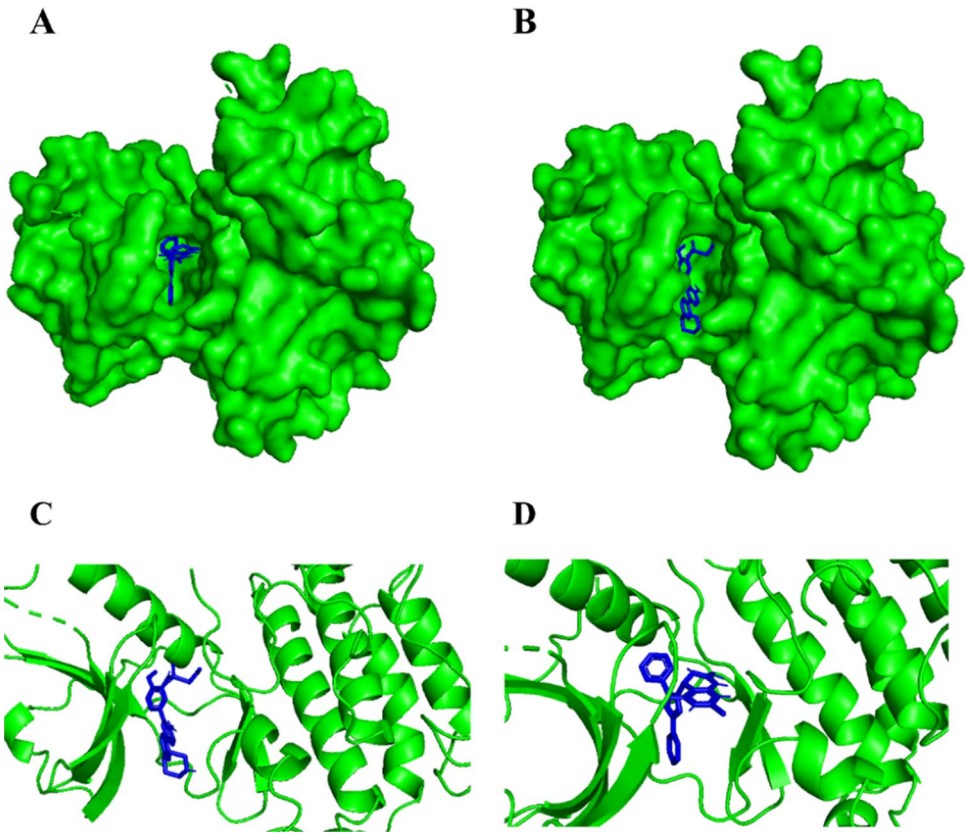

Fig. 3 Surface view of reference (**A**) and **4a** (**B**) and cartoon view of reference (**C**) and **4a** (**D**) interactions with the RIPK2

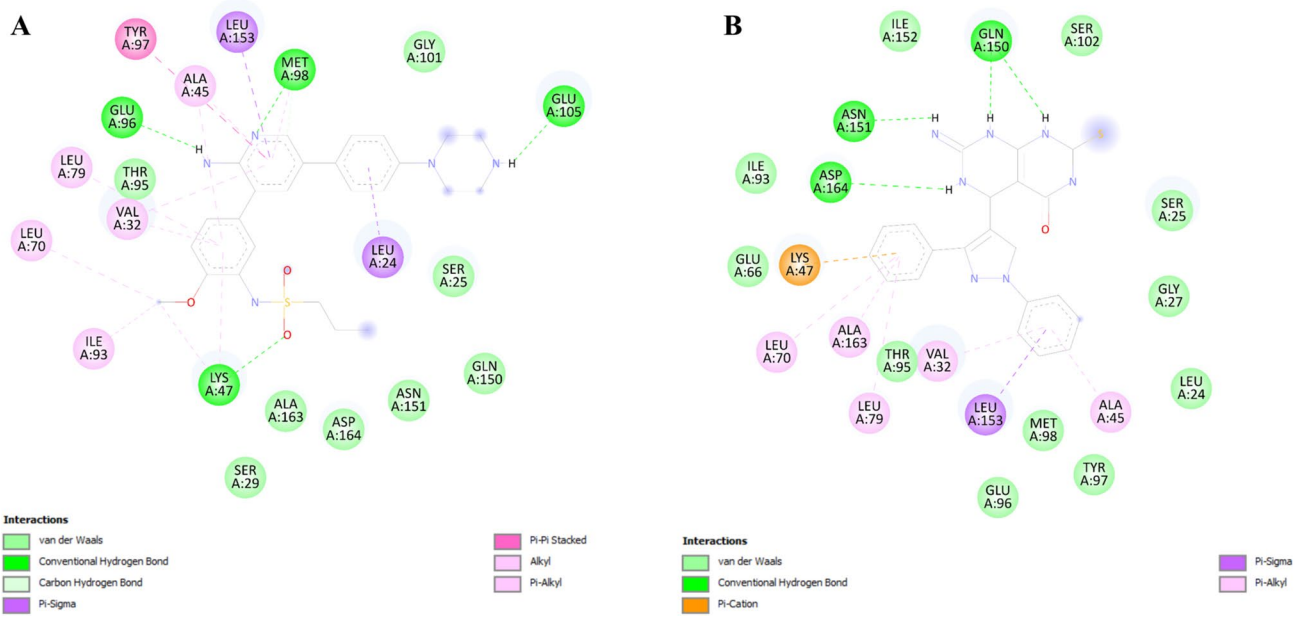

Fig. 4 **A** Protein–ligand interaction patterns of reference with RIPK2. **B** Protein–ligand interaction patterns of compound **4a** with RIPK2

in comparison with the reference compound were shown in Fig. 4A and B. The reference compound showed four hydrogen bonds (LYS47, GLU96, MET98, GLU105), seven van der Waals interactions and eight hydrophobic interactions in binding model analysis. The most active compound **4a** noticed four hydrogen bonds between residue GLN150,

ASN151 and ASP164 with NH groups of pyrimido[4,5-*d*] pyrimidine nucleus. Moreover, eleven van der Waals interactions and six hydrophobic interactions were noticed with the RIPK2 as shown Fig. 4B. Results of anticancer screening and of molecular docking comply with each other, conferring to which, compound **4a** was found to be the most potent ligand.

In-silico toxicity study

The toxicity parameters of the reference and the synthesized compounds were predicted using ADMETLAB 2.0. The human hepatotoxicity (H-HT), Drug-Induced Liver Injury (DIL1), AMES test, Rat Oral Acute Toxicity (ROAT), FDA Maximum recommended Daily Dose (FDAMDD), Agonistic effect against the Androgen receptor (NR-AR), Agonistic effect against the Estrogen receptor (NR-ER), activity towards peroxisome proliferator-activated receptor gamma (NR-PPAR-γ), antioxidant response element (SR-ARE), Carcinogenicity (CG), and Toxicophores (TX) of the reference as well as the synthesized compounds were predicted and tabulated in Table 5. It was evidence that compound **4a** showed less toxicity when compared to the reference compound and other compounds confirmed by H-HT, DILI, AMES, ROAT, and FDAMMD value ranges [32, 33]. The carcinogenicity and toxicophores values indicated that **4a** was less carcinogenic and had only two toxicophores which was less when compared to other derivatives. The NR-AR and NR-ER agonist values and the activities against the NR-PPAR-γ and SR-ARE also support that compound **4a** may become a potent ligand of choice with less toxic properties.

In-silico ADME study

The drug-likeness properties by Lipinski's rule and the ADME properties of the synthesized compounds as well as reference were evaluated. The molecular weight (MW) in g/mol, H-bond donor (HBD), H-bond acceptor (HBA), lipophilicity (log P), topological polar surface area (TPSA) in Å, Lipinski's evaluation, gastro-intestinal absorption (GIA), bioavailability (BA), and Pan-assay interference compounds

Table 5 Toxicity parameters of synthesized compounds

Compound	H-HT	DILI	AMES	ROAT	FDAMMD	NR-AR	NR-ER	NR-PPAR-γ	SR-ARE	CG	TX
Reference	0.981	0.998	0.546	0.506	0.98	0.013	0.040	0.567	0.894	0.78	3
4a	0.812	0.898	0.092	0.853	0.89	0.012	0.032	0.704	0.93	0.222	2
4b	0.932	0.993	0.365	0.772	0.941	0.025	0.004	0.011	0.555	0.609	3
4c	0.908	0.992	0.27	0.57	0.934	0.058	0.006	0.055	0.661	0.67	3
4d	0.906	0.991	0.249	0.57	0.937	0.013	0.01	0.357	0.731	0.638	3
4e	0.797	0.993	0.288	0.65	0.926	0.009	0.006	0.052	0.698	0.69	3
4f	0.935	0.993	0.932	0.725	0.917	0.008	0.012	0.028	0.85	0.905	2
4g	0.929	0.992	0.901	0.768	0.936	0.01	0.009	0.037	0.806	0.894	3
4h	0.862	0.993	0.155	0.864	0.951	0.008	0.006	0.019	0.629	0.74	3
4i	0.902	0.993	0.658	0.804	0.93	0.032	0.027	0.069	0.78	0.907	3
4j	0.819	0.993	0.204	0.51	0.924	0.013	0.006	0.017	0.733	0.775	3

0–0.3 (poor activity); 0.3–0.7 (medium activity); and 0.7–1.0 (high activity)

Table 6 Drug likeness and ADME properties of synthesized compounds

Compound	MW	HBD	HBA	Log P	TPSA	Lipinski	GIA	BA	PAINS
Reference	477.58	3	4	2.58	147.12	Yes	Low	0.55	No
4a	415.47	5	3	2.38	146.47	Yes	Low	0.55	No
4b	303.34	5	3	1.1	137.88	Yes	High	0.55	No
4c	319.34	6	4	0.72	158.11	No	Low	0.55	No
4d	319.34	6	4	0.75	158.11	No	Low	0.55	Yes
4e	289.31	6	3	0.72	148.88	No	Low	0.55	Yes
4f	318.31	5	4	0.52	174.47	Yes	Low	0.55	No
4g	318.31	5	4	0.53	174.47	Yes	Low	0.55	No
4h	307.76	5	2	1.62	128.65	Yes	High	0.55	No
4i	316.38	5	2	1.11	131.89	Yes	High	0.55	Yes
4j	289.31	6	3	0.71	148.88	No	Low	0.55	No

(PAINS) of the reference and synthesized compounds were depicted in Table 6. Out of ten evaluated synthesized compounds, only compounds **4a**, **4b**, **4f**, **4g**, **4h**, and **4i** have passed Lipinski's drug-likeness criteria. In further evaluation, compound **4i** was removed from the study due to the PAINS alert, which may lead to false positives [34], while all compounds and references showed similar bioavailability inside the body, the GI absorption varies depending on the peripheral functional group of compounds.

Structural activity relationship

Structure–activity relationship (SAR) studies describe that the alteration in the bio-activities of synthesized compounds purely depends upon the attached substituents (–R) and the nature of peripheral functional groups attached to them.

Anticancer SAR It was seen that the hetero-aromatic (pyrazole) aldehyde as a substitution compared to other aromatic aldehyde vastly elevated the anticancer activity against all the cancer types. It shows a good growth percent on active cancer cell lines. Moreover, the *para* substituted EDGs compound [–$N(CH_3)_2$, **4i**] displayed good anticancer activity against selected Colon, Renal and Melanoma cancer cell lines. Other EDGs and all EWGs substitutions on various positions of core nucleus were the possible reason for the diminution of the cancer activity.

Antimicrobial SAR The substitution of EWGs (–NO_2, –Cl) on *ortho*, *meta* and *para* positions were responsible for the elevation of antimicrobial activity, while pyrazole and EDGs substituted aldehyde were reason for the lower microbial potency (Fig. 5).

Conclusion

The present research aimed to evaluate synthesized pyrimido[4,5-*d*]pyrimidine motifs as anticancer and antimicrobial agents for drug discovery via green synthesis. Green metrics evaluation of the reaction was clearly evident that the reaction approach is ideal, green and sustainable. Additionally, the method was also simple and time efficient as the reaction time was only 5 min. Synthesized compounds (**4a–j**) were investigated for in-vitro anticancer primary screening for one dose against different cell lines of nine cancer types. The results displayed that the hetero-aromatic pyrazole substituted compound **4a** performed well as an anticancer agent with good mean growth percentage against active cancer cell lines. Compound **4i** exhibited good anticancer activity against Colon, Renal and Melanoma cancer cell lines. In-silico studies i.e., Molecular docking predictions suggested that compound **4a** has noteworthy binding energy (− 9.8 kcal/mol) and dissociation constant (0.54 µM). Drug-likeness and ADME properties also revealed the fewer

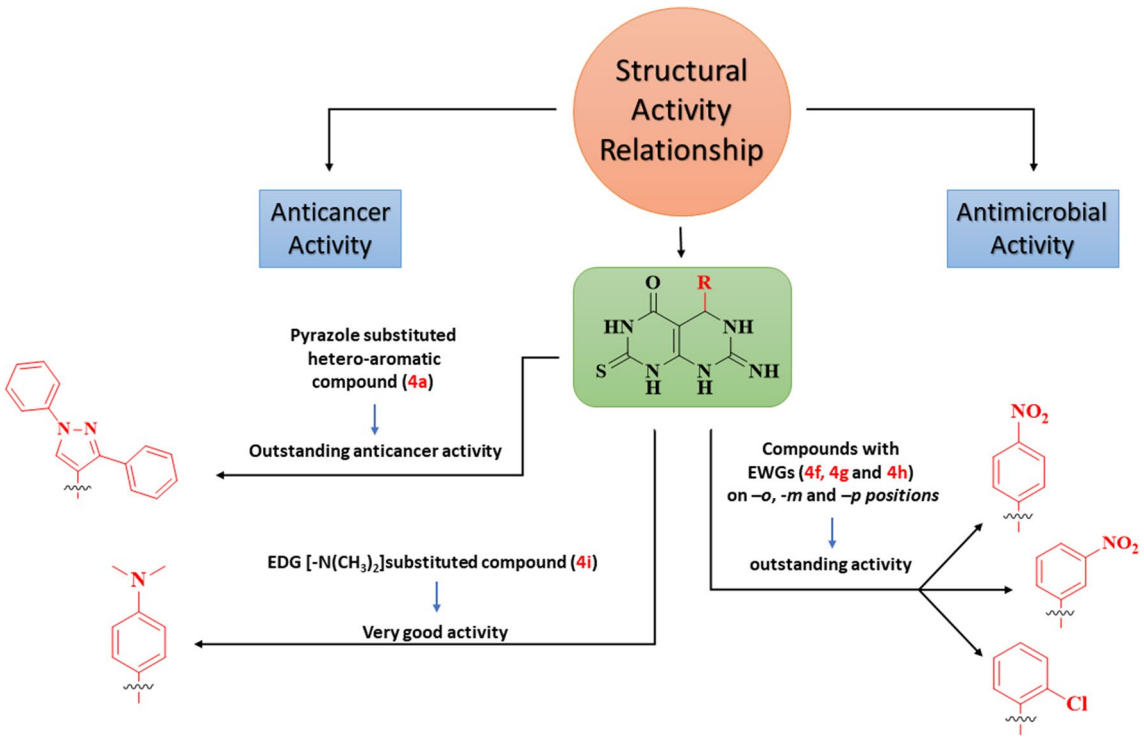

Fig. 5 SAR for anticancer and antimicrobial activity

toxic properties and potent inhibitory potential against the RIPK2 for compound **4a** in comparison with the reference. This result of in-vitro and in-silico studies concludes that compound **4a** can be potential candidate for future anticancer drug discovery. Moreover, antimicrobial screening data suggested that EWGs substituted derivatives **4f** (-4-NO_2), **4g** (-3-NO_2) and **4h** (-4-Cl) displayed good antimicrobial activity. Thus, synthesizing pyrimido[4,5-*d*]pyrimidine with the EWGs may act as a potential candidate after detailed optimization for antimicrobial agents.

Experimental section

Materials and physical measurements

The chemicals used were of AnalaR grade. ^{1}H-NMR and ^{13}C-NMR spectra were recorded on Bruker spectrometer [500 MHz (^{1}H) and 125 MHz (^{13}C)] using $CDCl_3$ as solvent and tetramethylsilane (TMS) as an internal standard. Measurements are displayed in parts per million (ppm). The IR spectra (ν, cm^{-1}) of all the motifs were recorded on a Perkin-Elmer FT-IR spectrophotometer using KBr. Mass spectra were recorded by SHIMADZU LC–MS spectrometer. Elemental analyses were performed on an ECS 4010 Elemental Combustion System and the resulting data were within the accepted range ($\pm$0.40) of the calculated values. M.P. were checked on an electro thermal melting point apparatus and were reported uncorrected. The completion of reaction and purity of compounds were checked on aluminum coated TLC plates 60 F245 (E. Merck) using methanol:chloroform (0.5:9.5 V/V) as mobile phase and visualized under ultraviolet (UV) light or in an iodine chamber.

General procedure for the synthesis of (5/7)-(aryl/heteroaryl)-7-imino-2-thioxo-2,3,5,6,7,8-hexahydropyrimido[4,5-*d*]pyrimidin-4(1*H*)-ones (4a–j)

A mixture of 2-thiobarbituric acid (0.01 mol) (**1**), guanidine (0.01 mol) (**2**) was taken in the flask. Then aldehyde derivatives (**3**) were added to the flask and the mixture was stirred for 2 min at room temperature. The iodine solution of 8 mol% was developed by dissolving iodine in potassium iodide solution made in water. Prepared iodine solution was dropwise added to the flask with continues stirring at room temperature. The flask was then placed in microwave (640 W) for 5 min at room temperature. The completion of the synthesis was monitored by TLC. The solid product was separated and washed thoroughly with sodium thiosulphate solution followed by sodium bicarbonate and water, dried and recrystallized from ethanol to afford the desired compound. The characterization data (FTIR, ^{1}H NMR, ^{13}C NMR, LCMS) of synthesized compounds (**4a–j**) are available in the supplementary [35].

5-(1,3-Diphenyl-1*H*-pyrazol-4-yl)-7-imino-2-thioxo-2,3,5,6,7,8-hexahydropyrimido[4,5-*d*]pyrimidin-4(1*H*)-one (4a)

Brown solid; Optimized %Yield: 84%; m.p. 253–254 °C; FTIR (KBr, cm^{-1}): 1110.97 (s, C–N), 1504.63 (w, C–H), 1597.13 (m, C=C), 1671.83 (m, C=N), 1705.18 (s, C=O), 3047.47 (m, 2° N–H); ^{1}H NMR (500 MHz, Chloroform) δ 11.81 (s, 1H), 8.51 (s, 1H), 7.85–7.75 (m, 2H), 7.63–7.41 (m, 8H), 7.41–7.32 (m, 1H), 6.05 (s, 1H), 4.08 (s, 1H), 2.34 (d, J = 12.2 Hz, 2H); ^{13}C NMR ($CDCl_3$, 125 MHz): δ 174.29, 165.17, 160.79, 154.30, 153.04, 139.97, 135.76, 131.08, 129.70, 128.62, 128.19, 128.03, 119.95, 118.21, 110.93, 38.47; LCMS: m/z 415.12 [M^+]; Anal. Calcd. for: $C_{21}H_{17}N_7OS$: C, 60.71; H, 4.12; N, 23.60; Found: C, 60.73; H, 4.15; N, 23.58%.

7-Imino-5-(4-methoxyphenyl)-2-thioxo-2,3,5,6,7,8-hexahydropyrimido[4,5-*d*]pyrimidin-4(1*H*)-one (4b)

Yellow solid; Optimized %Yield: 87%; m.p. 271–272 °C; FTIR (KBr, cm^{-1}): 1010.25 (s, C–O), 1295.90 (s, C–N), 1631.57 (m, C=C), 1623.10 (w, C–H), 1519.21 (s, C=O), 3465.58 (m, 2° N–H); ^{1}H NMR ($CDCl_3$, 500 MHz): δ 11.60 (s, 1H), 8.45 (s, 1H), 7.26 (d, J = 7.5 Hz, 2H), 6.91 (d, J = 7.3 Hz, 2H), 5.52 (s, 1H), 4.11 (s, 1H), 3.81 (s, 3H), 2.35 (s, 1H), 2.23 (s, 1H); ^{13}C NMR ($CDCl_3$, 125 MHz): δ 174.29, 159.21, 158.69, 153.34, 153.19, 131.12, 129.49, 113.50, 107.00, 56.03, 53.28; LCMS: m/z 303.08 [M^+]; Anal. Calcd. for: $C_{13}H_{13}N_5O_2S$: C, 51.47; H, 4.32; N, 23.09; Found: C, 51.49; H, 4.35; N, 23.10%.

5-(4-Hydroxy-3-methoxyphenyl)-7-imino-2-thioxo-2,3,5,6,7,8-hexahydropyrimido[4,5-*d*]pyrimidin-4(1*H*)-one (4c)

Light yellow solid; Optimized %Yield: 85%; m.p. 270–271 °C; FTIR (KBr, cm^{-1}): 1130.42 (s, C–O), 1270.41 (s, C–N), 1492.80 (m, C=C), 1612.84 (s, C=O), 1610.64 (w, C–H), 3202.24 (b, O–H), 3490.70 (m, 2° N–H); ^{1}H NMR ($CDCl_3$, 500 MHz): δ 11.64 (s, 1H), 8.49 (s, 1H), 6.95 (s, 1H), 6.75 (d, *J* = 7.6 Hz, 1H), 6.67 (d, *J* = 7.3 Hz, 1H), 5.57 (s, 1H), 4.13 (s, 1H), 3.89 (s, 3H), 3.51 (s, 1H), 2.38 (s, 1H), 2.26 (s, 1H); ^{13}C NMR ($CDCl_3$, 125 MHz): δ 174.29, 158.69, 153.88, 153.34, 148.03, 147.29, 132.08, 119.87, 115.76, 110.64, 107.00, 56.78, 53.18; LCMS: m/z 319.07 [M^+]; Anal. Calcd. for: $C_{13}H_{13}N_5O_3S$: C, 48.90; H, 4.10; N, 21.93; Found: C, 48.93; H, 4.12; N, 24.91%.

5-(2-Hydroxy-3-methoxyphenyl)-7-imino-2-thioxo-2,3,5,6,7,8-hexahydropyrimido[4,5-*d*]pyrimidin-4(1*H*)-one (4d)

Yellowish brown solid; Optimized %Yield: 83%; m.p. 280–281 °C; FTIR (KBr, cm^{-1}): 1330.40 (s, C–O), 1370.42 (s, C–N), 1401.76 (m, C=C), 1602.24 (s, C=O), 1589.44 (w, C–H), 3198.24 (b, O–H), 3475.61 (m, 2° N–H); ^{1}H NMR ($CDCl_3$, 500 MHz): δ 10.51 (s, 1H), 6.86–6.76 (m, 1H), 6.72–6.64 (m, 1H), 6.64–6.57 (m, 1H), 5.98 (s, 1H), 5.38 (s, 1H), 4.13 (s, 1H), 3.86–3.77 (m, 4H), 2.05 (s, 1H), 1.91 (s, 1H); ^{13}C NMR ($CDCl_3$, 125 MHz): δ 174.29, 159.05, 153.95, 153.34, 148.92, 147.68, 125.77, 122.41, 119.74, 114.87, 105.73, 56.78, 48.97; LCMS: m/z 319.07 [M^+]; Anal. Calcd. for: $C_{13}H_{13}N_5O_3S$: C, 48.90; H, 4.10; N, 21.93; Found: C, 48.91; H, 4.08; N, 24.90%.

5-(2-Hydroxyphenyl)-7-imino-2-thioxo-2,3,5,6,7,8-hexahydropyrimido[4,5-*d*]pyrimidin-4(1*H*)-one (4e)

Orange solid; Optimized %Yield: 86%; m.p. 286–287 °C; FTIR (KBr, cm^{-1}): 1398.31 (s, C–O), 1402.72 (m, C=C), 1452.73 (s, C–N), 1510.64 (s, C=O), 1640.74 (w, C–H), 2910.54 (b, O–H), 3098.71 (m, 2° N–H); ^{1}H NMR ($CDCl_3$, 500 MHz): δ 11.61 (s, 1H), 8.41 (s, 1H), 7.28 (s, 1H), 7.12–7.01 (m, 2H), 6.85 (dd, J = 11.1, 4.6 Hz, 2H), 6.04 (s, 1H), 4.12 (s, 1H), 2.33 (s, 1H), 2.23 (s, 1H); ^{13}C NMR ($CDCl_3$, 125 MHz): δ 174.29, 159.05, 156.55, 153.34, 153.10, 130.96, 130.32, 126.91, 119.81, 117.10, 105.73, 48.98; LCMS: m/z 289.06 [M^+]; Anal. Calcd. for: $C_{12}H_{11}N_5O_2S$: C, 49.82; H, 3.83; N, 24.21; Found: C, 49.85; H, 3.82; N, 24.20%.

7-Imino-5-(4-nitrophenyl)-2-thioxo-2,3,5,6,7,8-hexahydropyrimido[4,5-*d*]pyrimidin-4(1*H*)-one (4f)

Yellow solid; Optimized %Yield: 90%; m.p. 273–274 °C; FTIR (KBr, cm^{-1}): 1320.19 (s, C–N), 1522.01 (m, C=C), 1602.10 (s, C=O), 1580.20 (s, N=O), 1605.17 (w, C–H), 3138.10 (m, 2° N–H); ^{1}H NMR ($CDCl_3$, 500 MHz): δ 10.41 (s, 1H), 8.12 (d, J = 7.5 Hz, 2H), 7.46 (d, J = 7.5 Hz, 2H), 5.92 (s, 1H), 5.22 (s, 1H), 3.82 (s, 1H), 2.06 (s, 1H), 1.71 (s, 1H); ^{13}C NMR ($CDCl_3$, 125 MHz): δ 174.24, 158.63, 155.24, 153.28, 149.69, 148.83, 128.04, 123.20, 106.95, 53.23; LCMS: m/z 318.05 [M^+]; Anal. Calcd. for: $C_{12}H_{10}IN_6O_3S$: C, 45.28; H, 3.17; N, 26.40; Found: C, 45.30; H, 3.19; N, 26.44%.

7-Imino-5-(3-nitrophenyl)-2-thioxo-2,3,5,6,7,8-hexahydropyrimido[4,5-*d*]pyrimidin-4(1*H*)-one (4g)

Light cream solid; Optimized %Yield: 93%; m.p. 193–194 °C; FTIR (KBr, cm^{-1}): 1101.27 (s, C–N), 1440.12 (m, C=C), 1508.24 (s, C=O), 1602.25 (s, N=O), 1608.66 (w, C–H), 3598.14 (m, 2° N–H); ^{1}H NMR ($CDCl_3$, 500 MHz): δ 11.52 (s, 1H), 8.39 (s, 1H), 8.27 (d, J = 1.2 Hz, 1H), 8.07 (ddd, J = 4.6, 2.7, 1.4 Hz, 1H), 7.53–7.36 (m, 2H), 5.47 (s, 1H), 4.04 (s, 1H), 2.28 (s, 1H), 2.21 (s, 1H); ^{13}C NMR ($CDCl_3$, 125 MHz): δ 174.29, 158.69, 155.74, 153.34, 148.57, 141.97, 135.57, 130.19, 127.19, 126.66, 107.00, 53.18; LCMS: m/z 318.05 [M^+]; Anal. Calcd. for: $C_{12}H_{10}IN_6O_3S$: C, 45.28; H, 3.17; N, 26.40; Found: C, 45.27; H, 3.17; N, 26.41%.

5-(2-Chlorophenyl)-7-imino-2-thioxo-2,3,5,6,7,8-hexahydropyrimido[4,5-*d*]pyrimidin-4(1*H*)-one (4h)

Cream solid; Optimized %Yield: 89%; m.p. 188–189 °C; FTIR (KBr, cm^{-1}): 616.75 (s, C–Cl), 1401.08 (m, C=C), 1504.36 (s, C–N), 1625.10 (s, C=O), 1627.69 (w, C–H), 3045.82 (m, 2° N–H); ^{1}H NMR ($CDCl_3$, 500 MHz): δ 11.65 (s, 1H), 8.48 (s, 1H), 7.36 (dd, J = 7.4, 1.5 Hz, 1H), 7.17 (dtd, J = 28.6, 7.5, 1.4 Hz, 2H), 7.02 (dd, J = 7.4, 1.6 Hz, 1H), 6.08 (s, 1H), 4.08 (s, 1H), 2.47 (s, 1H), 2.33 (s, 1H); ^{13}C NMR ($CDCl_3$, 125 MHz): δ 174.29, 159.05, 155.74, 153.34, 139.91, 134.11, 131.80, 130.22, 129.35, 126.76, 105.73, 53.65; LCMS: m/z 307.03 [M^+]; Anal. calc for: $C_{12}H_{10}ClN_5OS$: C, 46.83; H, 3.28; N, 22.76; Found: C, 46.81; H, 3.25; N, 22.75%

5-(4-(Dimethylamino)phenyl)-7-imino-2-thioxo-2,3,5,6,7,8-hexahydropyrimido[4,5-*d*]pyrimidin-4(1*H*)-one (4i)

Red solid; Optimized %Yield: 91%; m.p. 295–296 °C; FTIR (KBr, cm^{-1}): 1329.18 (s, C–N), 1512.49 (w, C–H), 1517.12 (m, C=C), 1637.25 (m, C=N), 1654.17 (s, C=O), 3456.16 (m, 2° N–H); ^{1}H NMR ($CDCl_3$, 500 MHz): δ 10.40 (s, 1H), 7.07 (d, J = 7.3 Hz, 2H), 6.61 (d, J = 7.5 Hz, 2H), 5.95 (s, 1H), 4.98 (s, 1H), 3.85 (s, 1H), 2.92 (s, 6H), 2.08 (s, 1H), 1.72 (s, 1H); ^{13}C NMR ($CDCl_3$, 125 MHz): δ 174.29, 158.69, 155.24, 153.34, 151.82, 129.64, 127.85, 112.53, 107.00, 53.28, 41.91; LCMS: m/z 316.11 [M^+]; Anal. Calcd. for: $C_{14}H_{16}N_6OS$: C, 53.15; H, 5.10; N, 26.56; Found: C, 53.16; H, 5.13; N, 26.57%.

5-(4-Hydroxyphenyl)-7-imino-2-thioxo-2,3,5,6,7,8-hexahydropyrimido[4,5-*d*]pyrimidin-4(1*H*)-one (4j)

Green solid; Optimized %Yield: 82%; m.p. 307–308 °C; FTIR (KBr, cm^{-1}): 1390.89 (s, C–N), 1502.08 (s, C=O), 1602.11 (m, C=C), 1630.52 (w, C–H), 3030.98 (m, 2° N–H); ^{1}H NMR ($CDCl_3$, 500 MHz): δ 11.57 (s, 1H), 8.43 (s, 1H), 7.10 (d, J = 7.5 Hz, 2H), 6.77 (d, J = 7.5 Hz,

2H), 5.49 (s, 1H), 4.08 (s, 1H), 3.62 (s, 1H), 2.32 (s, 1H), 2.20 (s, 1H); ^{13}C NMR ($CDCl_3$, 125 MHz): δ 174.33, 158.72, 157.67, 153.37, 152.22, 131.33, 129.84, 115.63, 107.04, 53.32; LCMS: m/z 289.06 [M^+]; Anal. Calcd. for: $C_{12}H_{11}N_5O_2S$: C, 49.82; H, 3.83; N, 24.21; Found: C, 49.81; H, 3.85; N, 24.22%.

Green metrics assay

Concerning the principles of green chemistry, green chemistry metrics like atom economy, mass intensity and mass productivity are significant features of chemical processes. The major objective of these metrics is to accomplish efficient, simple, and eco-friendly synthetic protocol [36]. Hence, we prepared all motifs (**4a–j**) on a gram scale. With synthesizing compounds on a gram scale, we next estimated our chemical protocol on the "greenness" scale. These green chemistry metrics are calculated using the following formulas.

$$\%Atom\ Economy = \frac{M.W.\ of\ product}{\sum M.W.\ of\ all\ reactants\ used} \times 100$$

$$Mass\ Intensity = \frac{Total\ mass\ used\ in\ process\ step}{Mass\ of\ product}$$

$$Mass\ Productivity = \frac{1}{Mass\ Intensity} \times 100$$

Anticancer screening assay

In-vitro anticancer screening was evaluated under Developmental Therapeutics Program (DTP) at National Cancer Institute, Bethesda, USA. All the synthesized compounds (**4a–j**) were initially screened at a single high dose of 10^{-5} M concentration. The whole 60 human cancer cell lines were arranged into nine subpanels derived from nine different human cancer types; Leukemia, Non-Small Cell Lung Cancer, Colon, CNS, Melanoma, Ovarian, Renal, Prostate and Breast cancer cell lines. Results obtained from the single-dose screening were reported as a graph of the mean growth percent of the treated cells [37].

Molecular docking assay

The binding affinities of the synthesized compounds against the RIPK2 were evaluated through AutoDock Vina [38, 39]. The grid map points were set at 2.455 Å, − 29.315 Å, and 20.773 Å as in X, Y, and Z directions, respectively on the active site which includes LEU24, SER25, VAL32, ALA45, LYS47, LEU70, LEU79, ILE93, THR95, GLU96, TYR97, MET98, GLU105, GLN150, ASN151, LEU153, ALA163, ASP164 residues of the RIPK2. The point spacing was set as 0.375 Å with 10 runs and all the parameters were set default. The interaction complexes of RIPK2 with the synthesized compounds were visualized by Discovery studio visualizer and Pymol viewer.

Drug-likeness and ADME properties determination assay

The drug-likeness properties by Lipinski's rule of five and the Absorption, Distribution, Metabolism, and Excretion (ADME) properties of the synthesized compounds were predicted using the SwissADME server [40]. The molecule is said to be Lipinski passed when its molecular mass is below 500 Dalton, lipophilicity log P is less than 5 and H-bond donors & acceptors are below 5 and 10 respectively [41].

Toxicity prediction assay

The toxicity parameters of the reference compound and the synthesized compounds were evaluated using ADMETLAB 2.0 server [42]. The toxicity prediction enables the safety parameters and the pharmacodynamic properties of drug-like compounds.

Antimicrobial screening assay

The antimicrobial activity was evaluated as their minimum inhibitory concentration (MIC) by the Mueller Hinton Broth dilution method [43]. The antimicrobial activity of synthesized molecules (**4a–j**) was tested as opposed to the following microorganisms: Gram (−) ve bacteria (*E. coli* [MTCC-1687] and *S. marcescens* [MTCC 4822]), Gram (+) ve bacteria (*S. epidermidis* [MTCC-435] and *S. pyogenes* [MTCC-442]) and Fungi (*A. niger* [MTCC-282] and *F. solani* [MTCC-9174]). The synthesized motifs were screened for their antimicrobial activity in triplicate sets against these microbes at several concentrations of 2500–200 µg/mL. The compounds which were found to be active in primary analysis were further diluted and evaluated. 50, 25, 12.5 and 10 µg/mL suspensions were further inoculated on appropriate media and the growth was noticed after 1 or 2 days. In this study, Chloramphenicol, Ciprofloxacin and Nystatin were used as the standard drugs for the estimation of the activity.

Supplementary Information The online version contains supplementary material available at https://doi.org/10.1007/s11030-023-10712-9.

Acknowledgements The authors are thankful to the Department of Chemistry, C. U. Shah University, Surendranagar and the Department

of Chemistry, RK University, Rajkot for supporting the research. The authors gratefully acknowledge the support of in-vitro anticancer analyses from the National Cancer Institute (NIH), Bethesda, USA and Mr. Dashrath Kanzariya, PDEU, Gandhinagar for spectral analyses.

Author contributions HDT performed the synthesis, characterization and biological assay of compounds and also prepared the manuscript. GI performed a molecular docking study and analyzed the results. PSR performed ADMET study and analyzed the results. SDH analyzed the anticancer and antimicrobial data and gave valuable input in the result discussion. BYP contributed to the design, characterized the compounds, supported the preparation of the manuscript, and also supervised all phases of the study.

Funding This work was funded by "ScHeme Of Developing High quality research (SHODH)" Scholarship (202001260001), Department of Education, Gujarat Government, India.

Declarations

Conflict of interest The authors declare that they have no conflict of interest.

References

1. Siegel RL, Miller KD, Wagle NS, Jemal A (2023) Cancer statistics. CA Cancer J Clin 73(1):17–48. https://doi.org/10.3322/caac.21763
2. Hadiyal SD, Parmar ND, Kalavadiya PL, Lalpara JN, Joshi HS (2020) Microwave-assisted three-component domino synthesis of polysubstituted 4H-pyran derivatives and their anticancer activity. Russ J Org Chem 56:671–678. https://doi.org/10.1134/S1070428020040168
3. Torre LA, Islami F, Siegel RL, Ward EM, Jemal A (2017) Global cancer in women: burden and trendsglobal cancer in women: burden and trends. Cancer Epidemiol Biomark Prev 26(4):444–457. https://doi.org/10.1158/1055-9965.EPI-16-0858
4. Zhou H, Lv S, Zhang D, Deng M, Zhang X, Tang Z et al (2018) A polypeptide based podophyllotoxin conjugate for the treatment of multi drug resistant breast cancer with enhanced efficiency and minimal toxicity. Acta Biomater 73:388–399. https://doi.org/10.1016/j.actbio.2018.04.016
5. Bhaskar VH, Mohite PB (2010) Synthesis, characterization and evaluation of anticancer activity of some tetrazole derivatives. J Optoelectron Biomed Mater 2(4):249–259
6. Patel BY, Karkar TJ, Bhatt MJ (2021) Synthesis of 5-substituted-1,3,4-oxadiazole clubbed pyrazole and dihydropyrimidine derivatives as potent bioactive agents. Eur Chem Bull 10(1):13–20. https://doi.org/10.17628/ecb.2021.10.13-20
7. Desai NC, Pandya MR, Patel BY, Bhatt MJ, Karkar TJ (2016) Synthesis of novel N,N-dimethyl-1-(5-methyl-2-arylimidazo[1,2-a]pyridin-3-yl) methanamine derivatives as potential antimicrobial agents. Indian J Chem 55B(09):1136–1143
8. Desai NC, Bhatt N, Dodiya A, Karkar T, Patel B, Bhatt M (2016) Synthesis, characterization and antimicrobial screening of thiazole based 1,3,4-oxadiazoles heterocycles. Res Chem Intermed 42:3039–3053. https://doi.org/10.1007/s11164-015-2196-x
9. Desai NC, Shihory N, Bhatt M, Patel B, Karkar T (2015) Studies on antimicrobial evaluation of some 1-((1-(1*H*-benzo[*d*]imidazol-2-yl)ethylidene)amino)-6-((arylidene)amino)-2-oxo-4-phenyl-1,2-dihydropyridine-3,5-dicarbonitriles. Synth Commun 45(23):2701–2711. https://doi.org/10.1080/00397911.2015.1102286
10. Desai NC, Vaghani HV, Patel BY, Karkar TJ (2018) Synthesis and antimicrobial activity of fluorine containing pyrazole-clubbed dihydropyrimidinones. Indian J Pharm Sci 80(2):242–252. https://doi.org/10.4172/pharmaceutical-sciences.1000351
11. Trivedi HD, Patel BY, Patel PK, Sagar SR (2022) Synthesis, molecular modeling, ADMET and fastness studies of some quinoline encompassing pyrimidine azo dye derivatives as potent antimicrobial agents. Chem Data Collect 41:100923. https://doi.org/10.1016/j.cdc.2022.100923
12. Trivedi HD, Joshi VB, Patel BY (2023) Quinoline incorporating pyrimidine heterocyclic azo dye derivatives: synthesis, characterization and applications. Indian J Chem 62(4):380–392. https://doi.org/10.56042/ijc.v62i4.425
13. Desai NC, Patel BY, Jadeja KA, Dave BP (2017) Landscaping of quinoline based heterocycles as potential antimicrobial agents: a mini review. NAPDD 1(4):64–67. https://doi.org/10.56042/ijc.v62i4.425
14. Sridhara MB, Rakesh KP, Manukumar HM, Shantharam CS, Vivek HK, Kumara HK, Mohammed YHE, Gowda DC (2020) Synthesis of dihydrazones as potential anticancer and DNA binding candidates: a validation by molecular docking studies. Anti-Cancer Agents Med Chem 20(7):845–858
15. Rakesh KP, Darshini N, Manukumar HM, Vivek HK, Eissa MY, Prasanna DS, Mallesha N (2018) Xanthone conjugated amino acids as potential anticancer and DNA binding agents: molecular docking, cytotoxicity and SAR studies. Anti-Cancer Agents Med Chem 18(15):2169–2177
16. Moku B, Ravindar L, Rakesh KP, Qin HL (2019) The significance of N-methylpicolinamides in the development of anticancer therapeutics: synthesis and structure-activity relationship (SAR) studies. Bioorg Chem 86:513–537
17. Zhang X, Rakesh KP, Bukhari SNA, Balakrishna M, Manukumar HM, Qin HL (2018) Multi-targetable chalcone analogs to treat deadly Alzheimer's disease: current view and upcoming advice. Bioorg Chem 80:86–93
18. Zhang X, Rakesh KP, Shantharam CS, Manukumar HM, Asiri AM, Marwani HM, Qin HL (2018) Podophyllotoxin derivatives as an excellent anticancer aspirant for future chemotherapy: a key current imminent need. Bioorg Med Chem 26(2):340–355
19. Dong P, Rakesh KP, Manukumar HM, Mohammed YHE, Karthik CS, Sumathi S, Qin HL (2019) Innovative nano-carriers in anticancer drug delivery—a comprehensive review. Bioorg chem 85:325–336
20. Trivedi HD, Joshi VB, Patel BY (2022) Pyrazole bearing pyrimidine analogues as the privileged scaffolds in antimicrobial drug discovery: a review. Anal Chem Lett 12(2):147–173. https://doi.org/10.1080/22297928.2021.1910565
21. Desai NC, Vaghani HV, Karkar TJ, Patel BY, Jadeja KA (2017) Synthesis and antimicrobial studies of 1,2,3,4-tetrahydropyrimidine bearing imidazole analogues. Indian J Chem 56(1):438
22. Desai NC, Patel BY, Dave BP (2016) Approach for the synthesis of potent antimicrobials containing pyrazole, pyrimidine and morpholine analogues. Int Lett Chem Phys Astron 69:87–96. https://doi.org/10.18052/www.scipress.com/ILCPA.69.87
23. Xu J, Chmela V, Green NJ, Russell DA, Janicki MJ, Góra RW et al (2020) Selective prebiotic formation of RNA pyrimidine and DNA purine nucleosides. Nature 582(7810):60–66. https://doi.org/10.1038/s41586-020-2330-9
24. Venkatesh T, Bodke YD, Nagaraj K, Kumar SR (2018) One-pot synthesis of novel substituted phenyl-1,5-dihydro-2*H*-benzo[4,5]thiazolo[3,2-*a*]pyrimido[4,5-*d*]pyrimidine derivatives as potent antimicrobial agents. Med Chem 8:1–7. https://doi.org/10.4172/2161-0444.1000488

25. Santosh R, Paul P, Selvam MK, Raril C, Krishna PM, Manjunatha JG et al (2019) One-pot synthesis of pyrimido [4,5-*d*]pyrimidine derivatives and investigation of their antibacterial, antioxidant, DNA-binding and voltammetric characteristics. ChemistrySelect 4(3):990–996. https://doi.org/10.1002/slct.201803416
26. Grewal A, Kumar K, Redhu S, Bhardwaj S (2013) Microwave assisted synthesis: a green chemistry approach. Int Res J Pharm App Sci 3:278–285
27. Shi F, Zhou D, Tu S, Li C, Cao L, Shao Q (2008) Pot, atom and step economic synthesis of fused three heterocyclic ring compounds under microwave irradiation in water. J Heterocycl Chem 45(5):1305–1310. https://doi.org/10.1002/jhet.5570450508
28. Lalpara JN, Hadiyal SD, Radia AJ, Dhalani JM, Dubal GG (2022) Design and rapid microwave irradiated one-pot synthesis of tetrahydropyrimidine derivatives and their screening in vitro antidiabetic activity. Polycycl Aromat Compd 42(6):3063–3078. https://doi.org/10.1080/10406638.2020.1852586
29. Liandi AR, Cahyana AH, Kusumah AJF, Lupitasari A, Alfariza DN, Nuraini R et al (2023) Recent trends of spinel ferrites (MFe_2O_4: Mn Co, Ni, Cu, Zn) applications as an environmentally friendly catalyst in multicomponent reactions: a review. CSCEE. https://doi.org/10.1016/j.cscee.2023.100303
30. Alsharif Z, Ali MA, Alkhattabi H, Jones D, Delancey E, Ravikumar PC, Alam MA (2017) Hexafluoroisopropanol mediated benign synthesis of 2*H*-pyrido[1,2-*a*]pyrimidin-2-ones by using a domino protocol. New J Chem 41(24):14862–14870
31. Castro-Puyana M, Marina ML, Plaza M (2017) Water as green extraction solvent: principles and reasons for its use. Curr Opin Green Sustain Chem 5:31–36. https://doi.org/10.1016/j.cogsc.2017.03.009
32. Mekala JR, Ramalingam PS, Mathavan S, Yamajala RB, Moparthi NR, Kurappalli RK et al (2022) Synthesis, in vitro and structural aspects of cap substituted suberoylanilide hydroxamic acid analogs as potential inducers of apoptosis in glioblastoma cancer cells via HDAC/microRNA regulation. Chem Boil Interact 357:109876. https://doi.org/10.1016/j.cbi.2022.109876
33. Mekala JR, Kurappalli RK, Ramalingam P, Moparthi NR (2021) *N*-acetyl l-aspartate and triacetin modulate tumor suppressor microRNA and class I and II HDAC gene expression induce apoptosis in glioblastoma cancer cells in vitro. Life Sci 286:120024. https://doi.org/10.1016/j.lfs.2021.120024
34. Parasuraman S (2011) Toxicological screening. J Pharmacol Pharmacother 2(2):74. https://doi.org/10.4103/0976-500X.81895
35. Trivedi HD, Joshi VB, Patel BY (2023) Water mediated pot, atom, and step economic (PASE) synthesis of pyrimido[4,5-*d*] pyrimidines using ultrasound and microwave irradiation approaches. Synth Commun. https://doi.org/10.1080/00397911.2023.2199358
36. Arafa WAA, Faty RAM, Mourad AK (2018) A new sustainable strategy for synthesis of novel series of bis-imidazole and bis-1,3-thiazine derivatives. J Heterocycl Chem 55(8):1886–1894. https://doi.org/10.1002/jhet.3221
37. Hadiyal SD, Lalpara JN, Parmar ND, Joshi HS (2022) Microwave irradiated targeted synthesis of pyrrolobenzodiazepine embrace 1,2,3-triazole by click chemistry synthetic aspect and evaluation of anticancer and antimicrobial activity. Polycycl Aromat Compd 42(7):4752–4768. https://doi.org/10.1080/10406638.2021.1913425
38. Trott O, Olson AJ (2009) AutoDock Vina: improving the speed and accuracy of docking with a new scoring function, efficient optimization and multithreading. J Comput Chem 31:455–461. https://doi.org/10.1002/jcc.21334
39. Ramalingam PS, Balakrishnan P, Rajendran S, Jothi A, Ramalingam R, Arumugam S (2023) Identification of dietary bioflavonoids as potential inhibitors against KRAS G12D mutant—novel insights from computer-aided drug discovery. Curr Issues Mol Biol 45(3):2136–2156. https://doi.org/10.3390/cimb45030137
40. Daina A, Michielin O, Zoete V (2017) SwissADME: a free web tool to evaluate pharmacokinetics, drug-likeness and medicinal chemistry friendliness of small molecules. Sci Rep 7(1):42717. https://doi.org/10.1038/srep42717
41. Lipinski CA, Lombardo F, Dominy BW, Feeney PJ (1997) Experimental and computational approaches to estimate solubility and permeability in drug discovery and development settings. Adv Drug Deliv Rev 23(1–3):3–25. https://doi.org/10.1016/s0169-409x(00)00129-0
42. Xiong G, Wu Z, Yi J, Fu L, Yang Z, Hsieh C et al (2021) ADMETlab 2.0: an integrated online platform for accurate and comprehensive predictions of ADMET properties. Nucleic Acids Res 49(W1):W5-14. https://doi.org/10.1093/nar/gkab255
43. Desai NC, Patel BY, Dave BP (2017) Synthesis and antimicrobial activity of novel quinoline derivatives bearing pyrazoline and pyridine analogues. Med Chem Res 26:109–119. https://doi.org/10.1007/s00044-016-1732-6

Authors and Affiliations

Harsh D. Trivedi[1] · Bonny Y. Patel[2] · Sanjay D. Hadiyal[3] · Gopal Italiya[4] · Prasanna Srinivasan Ramalingam[4]

✉ Bonny Y. Patel
bonny.y.patel@gmail.com

[1] Department of Chemistry, B.V. Shah (Vadi-Vihar) Science College, C.U. Shah University, Wadhwan City, Gujarat 363001, India

[2] Department of Chemistry, School of Science, RK University, Rajkot, Gujarat 360020, India

[3] Department of Chemistry, Atmiya University, Rajkot, Gujarat 360005, India

[4] School of Bio Science and Technology (SBST), Vellore Institute of Technology, Vellore, Tamil Nadu, India